The Nucleus **50**, No. 3 (2013) 189-207

The Nucleus
A Quarterly Scientific Journal of Pakistan Atomic Energy Commission
NCLEAM, ISSN 0029-5698

EFFECT OF MATERIAL FLAWS ON THE MODAL PARAMETERS OF ISOTROPIC MATERIAL USING GROUND VIBRATION TESTING

*A. MUNIR, S. KHUSHNOOD[1] and N. AHMED

Centre for Engineering Sciences and Technology (CESAT), Islamabad, Pakistan

[1]University of Engineering and Technology, Taxila, Pakistan

(Received May 20, 2013 and accepted in revised form August 19, 2013)

Modes are inherent properties of a structure, and are determined by the material properties (mass, damping, and stiffness), and boundary conditions of the structure. Experimental and numerical Ground vibration testing of the low carbon steel plate has been performed to study the changes in modal parameters (modal frequencies, mode shapes, mass, stiffness and damping) either by the load distribution or by material flaws like voids, cracks and porosity etc. Delicacies in experimental Ground vibration testing based on experimental experience are explained to define a methodology for precise experimental testing in order to avoid experimental uncertainties. The difference in numerical and experimental results is also discussed along with reasoning in order to estimate the accuracy of numerical and experimental results. The changes in natural frequencies and mode shapes have been studied for different cases. The cracks, holes and different masses have been induced in the plate and the shift of modal parameters was observed due to single flaw and the combination of flaws in order to estimate the effect of uncertainties in ground Vibration testing. After this research, it is concluded that due to material flaws the stiffness of the material changes, which ultimately affect the modal parameters. Due to change in modal parameters, Aeroelastic Analysis (Flutter speed) also changes, which might result as catastrophic failure of the structure.

Keywords: Experimental modal analysis, MSC Nastran 2008, Ground vibration test, Cracks and holes, Materials flaws, Uncertainties due to material flaws.

Nomenclature

B_{hh} = Modal damping matrix

c = Mean Aerodynamic Chord Length (m)

F = Force (N)

f_i = Natural Frequency (Hz)

fs = Sampling Frequency (Hz)

f(max) = Maximum Frequency (Hz)

f_N = Natural Frequency (Hz)

Δf = Frequency (Hz)

K_{hh} = Modal Stiffness Matrix

[K] = Stiffness Matrix

L = Length (m)

M = Mass (Kg)

M_{hh} = Modal Mass Matrix

[M] = Mass Matrix

Q^{I}_{hh} = Generalized Aerodynamic Damping Matrix

Q^{R}_{hh} = Generalized Aerodynamic Stiffness Matrix

T = Time Period (s)

R = Mode

s = Mode

u_h = Modal Displacements

V = Airspeed (m/s)

X = Displacement (m)

X' = Amplitude (m)

ω = Circular Natural Frequency (rad/s)

ρ = Air density (Kg/m^3)

{Φ} = Eigenvector or Mode Shape

TFA = Time Frequency Analysis

FFT = Fast Fourier Transform

GVT= Ground Vibration Testing

FEM= Finite Element Method

1. Introduction

Modes are inherent properties of a structure, and are determined by the material properties (mass, damping and stiffness) and boundary conditions of the structure. Modes are greatly affected by material and structural flaws because it

* Corresponding author : azharmunir@hotmail.com

changes the modal parameters. Modal analysis is an emerging tool applied for the first in 1940 to evaluate the modal parameters of the structures and in the next two decades development was slow known as the mechanical impedance era. The modern era of modal analysis are the last 30 years, based upon the commercial availability of the first Fourier transform (FFT) spectrum analyzer, TFA and the discrete acquisition and analysis of data, together with the availability of increasingly smaller, less expensive and more powerful digital computers to process the data [1-8]. Modal parameters may be determined analytically using finite element method (FEM) or experimentally using different experimental techniques. The majority of structures can be made to resonate. Resonant vibration is caused by an interaction between the inertial and elastic properties of the materials within a structure. For structural vibration problem, the resonances of a structure are identified and quantified [9-10].

The field of structural dynamics addresses the dynamic deformation behavior of continuous structural configurations and covers the determination of natural frequencies and mode shapes, response due to initial conditions, generalized mass, generalized stiffness, forced response in the time domain and frequency response and the field of aero-elasticity describes the interaction of aerodynamic, inertia and elastic forces for a flexible structure [11]. Structural dynamic phenomena can result in dangerous static and dynamic deformations and instabilities which further lead to the failure of structure. Such deformations and instabilities have very important practical consequences in many areas of technology [12]. The solution of many structural dynamics problems is a basic requirement for achieving an operationally reliable and structurally optimal system [13].

It is impossible to prevent the initiation and propagation of cracks [14]. As one of the failure modes for the high-strength materials, crack initiation and propagation due to the manufacturing process or fatigue and impact loading during service has long been an important topic in engineering materials and fracture mechanics communities [15]. The initiation of cracks in wing structure is not unusual as they may be produced by either by manufacturing, molding, fatigue, or impact damage and propagation of the crack is often due to the low and high frequency vibration in the structure [16-17].

Evaluation of modal parameters of plates specifically with cracks is not a new study. D. R. Perchard and A.S.J. Swamidas generated a finite element model of the structure, a slender cantilever plate using an integrated software package, SDRC IDEAS, to estimate the changes in various modal parameters, caused by B notch type crack [18]. Theoretical studies were carried out by Solecki [19-21] on rectangular plates with cracks parallel or inclined to supporting sides; the cracks were through the thickness cracks. S. H. Yoo and H.K. Kwak suggested a new method to enhance the sensitivity of the ADSM in crack location. These methods are applied to identify the crack existence and locations in rectangular thin plate using strain mode shapes [22]. It is apparent that the strain mode shapes are more sensitive than displacement mode shapes for identification of a crack from literature survey [23]. The MAC [24] (Modal Assurance Criteria) and The IMAC [25] (Inverse MAC) are used first to detect and locate a crack.

R. Kolar studied the modal characteristics of isotropic plates with damage identified as cracks using FEM in MSC Nastran [26].

In the previous research work, structural dynamic uncertainties studies due to crack, holes, mass distribution (Symmetric and Asymmetric) and manufacturing flaws were individually carried out by analytical, numerical and experimental techniques on different engineering materials but the combination of such uncertainties had never been focused on isotropic materials. Even such individually carried out studies never quantify the combine effect of such uncertainties on isotropic materials. In this research work, structural dynamic uncertainties due to the material flaws and mass distribution was studied on a low carbon steel plate by assuming it as a wing of an aircraft (Isotropic Material). A simple plate with assumption that no flaw in it, is taken and modal analysis is performed both numerically and experimentally. Then material and structural flaws like cracks, holes were induced and symmetric and asymmetric lumped masses were attached step by step to see the individual as well as the cumulative effects of the flaws on structural dynamic parameters both numerically and experimentally. Individual and cumulative variation in the modal parameters due to individual and combination of structural flaws, and symmetric and asymmetric lumped masses attachment were analyzed on four critical modes; first bending, first torsion, second bending and second torsion. A significant shift in modal

parameters has been observed which shows that material flaws produce uncertainty in the results and these uncertainties should be incorporated at the initial design stage in order to avoid sudden failures.

2. FEM Model and Results

A low carbon steel plate is chosen with the dimensions as shown in Figure 1. In the model finite element model (FEM) based software, MSC Nastran 2008 is used. The specifications of this model are given in Table 1.

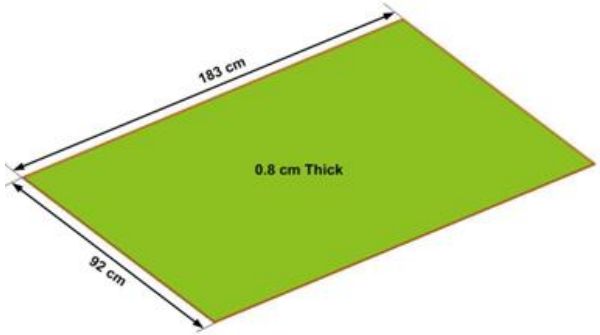

Figure 1. Low carbon steel plate.

Table 1. Material properties of low carbon steel plate.

No	Material Properties		Dimensions	
1	Mass	104 kg	Length	183 cm
2	Modulus of Elasticity	210 G Pa	Width	92 cm
3	Density	7800 kg / m^3	Thickness	0.8 cm

The element type 2D shell (quads 4) is taken and a mesh size of 25 X 25 mm is selected for a single element. The total numbers of elements are 2701 as shown in Figure 2. From 0 to 120 Hz, 10 modes are extracted using reduced form of equation of motion as in equation 1 in Nastran solution SOL103 [27] where no damping and no applied loading are considered.

Block Lenczos algorithm [1] with free-free boundary conditions to the structure is used.

$$[M]\{\ddot{u}\} + [K]\{u\}=0 \quad (1)$$

where [M] is mass matrix, [K] is stiffness matrix, {u} assumes a harmonic solution ($\{u\}=\{\Phi\}\sin \omega t$), {Φ} is the eigenvector or mode shape and ω is the circular natural frequency.

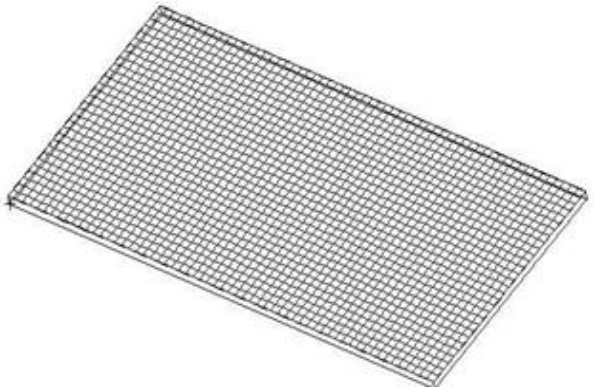

Figure 2. FEM model of plate.

Solutions of the reduced form of the equation of motion [1] as shown in equation 2 are:

$$[[K]- \omega_i^2[M]]\{ \Phi_i\}=0 , \quad \text{i.e. } i = 1,2,3, \quad (2)$$

The results of equation are eigenvalues i=1,2,3,….. and eigenvectors which define mode shape of structure and are in relation with natural frequency [1] as shown in equation 3, for certain modes:

$$f_{i=} \omega_i/2\pi \quad (3)$$

where, f_i is the natural frequency.

The numerical results are shown in Table 2.

The lower frequency modes are important for dynamic analysis i.e. first bending, first torsion, second bending and second torsion modes [28]. First four modes are discussed for further comparison purpose as shown in Figure 3.

3. Ground Vibration Testing (GVT) With Delicacies

Ground Vibration Testing is a process in which metallic structure is represented in term of its dynamic characteristics i.e. natural frequencies, damping factors, modes shapes, generalized mass and stiffness. It is almost similar to the experimental modal analysis with few additional things. There are two commonly known modal analysis methods being used for structural dynamic analysis namely sine dwell method and frequency response function method (FRF). Selection of the method and acquisition of reliable results depend on the understanding of following practical concepts.

Table 2. Numerical results.

No.	Modes	Numerical Modes (Hz)	Mode shape
1	1	12.80	First Bending
2	2	15.738	First Torsion
3	3	25.7	Asymmetric Torsion
4	3	34.44	Second Bending
5	4	35.534	Second Torsion
6	5	51.86	Asymmetric Second Bending
7	6	60.155	Symmetric Second Twist
8	8	70.702	Symmetric Third bending
9	9	86.051	Symmetric Third Torsion
10	10	94.969	Asymmetric Fourth Bending

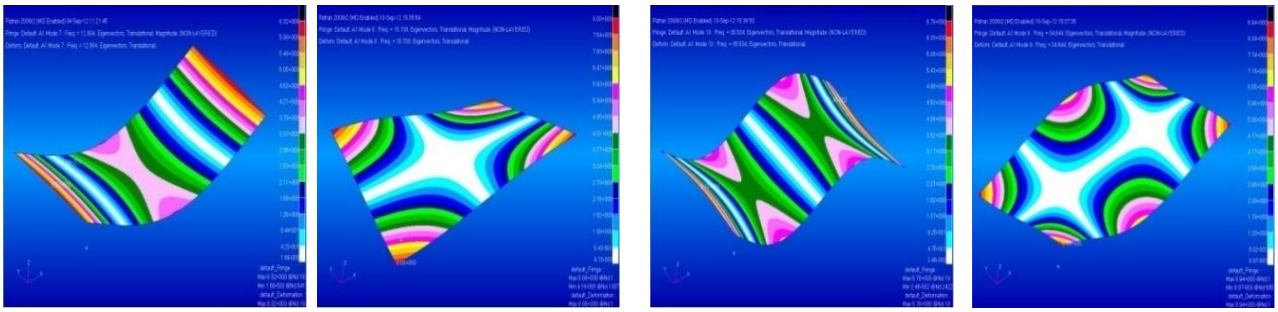

Mode 1: 1st Bending Mode 2: 1st Torsion Mode 3: 2ndBending Mode 4: 2nd Torsion

Figure 3. Mode shapes of low carbon steel plate.

In sine dwell method only one frequency is excited by sinusoidal force during the observation period. Natural mode is isolated by sweeping the frequency/force level such that the forcing function is orthogonal to all but the mode of interest. For isolating or tuning mode using multi shaker techniques, the force is adjusted on the individual shakers/exciter at the natural frequency, until the acceleration response at all the measurement points is in quadrature with the excitation forces. Use Lissajious figures which is quite convenient in this regard. Difficulties arise when a large number of shakers/exciters are used to isolate modes in frequency range of high modal density. Different methods are used to automate the force appropriation task. Deck's method is most widely used, which is based on minimizing the velocity amplitude response by adjusting the force and frequency levels [29]. The sine dwell method is being mostly used for complex structures for it accurate isolation of modes, close modal parameter estimation, more sophistication in the test setup and minimal data acquisition capabilities. However, more post processing of the acquired data, time consuming/lengthy and large number of shakers/exciters requirement are its demerits.

FRF method describes the input-output (force response) relationships of any system and is simply a ratio of response to excitation. Modal parameters are estimated from FRF and the modal parameters are as accurate as estimated from FRF. This method is used for impulse excitation

only [30]. This function depends upon the structure and not on the excitation level. In this way mode shape can be computed. FRF is maximum at the natural Frequency and displacement is in quadrature with the force.

The excitation techniques used for FRF method are SISO (single input single output), SIMO (single input multiple output), MISO (multiple input single output) and MIMO (multiple input multiple output).

MIMO is the best testing situation since the data is collected in the shortest possible time with fewest changes in the test condition [30]. FRF method is the quickest, easiest way to estimate parameters, perform simply using an impact hammer and give good modes identification with less accurate modal parameters estimation.

The results of numerical model of the plate using MSC Nastran 2008 are further investigated experimentally through multiple point excitation system and multiple accelerometer system using the Ground vibration testing setup as shown in Figures 4, 5 and 6.

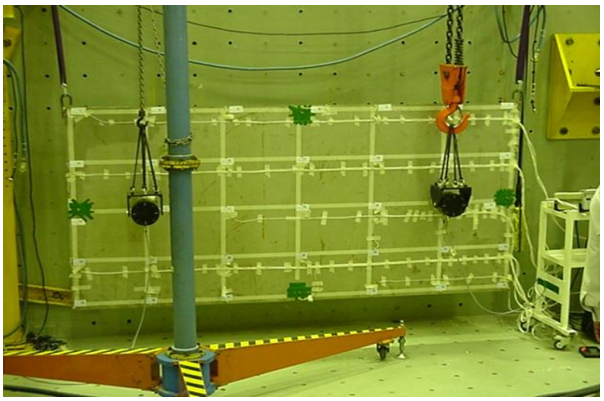

Figure 4. Experimental modal analysis setup.

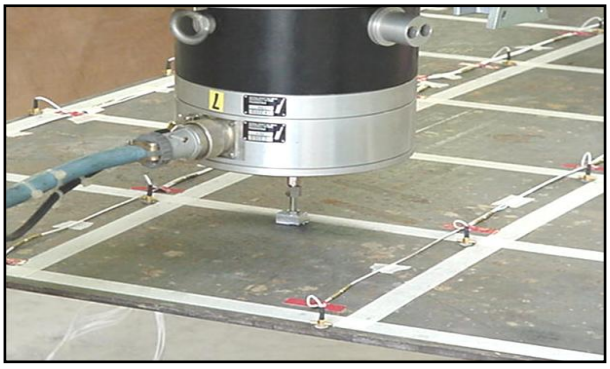

Figure 5. Experimental modal analysis setup.

The necessary steps in Ground vibration testing are assumptions, structure mounting for free-free boundary conditions, experimental model in modal software, sensor calibration and mounting on structure, installation of excitation system, acquisition system, signal processing, modal data validation, modal data presentation and frequency response analysis. Step by step all setup is explained below alongwith delicacies in order to get precise results of experimental modal analysis.

3.1. Assumptions

The structure is assumed to be linear i.e. amplitude of the response varies linearly with the magnitude of applied force and natural frequency is independent of the magnitude of the force. The assumption helps in using simplest mathematical and computational models. The force range is selected such that the structure behaves linearly and used for the mode isolation and parameter estimation.

Input output measurements contain enough information to generate an adequate behavioral model of the structure.

Experimental method, equipment and condition are properly set as per requirement of the modal density of the structure. Modal density (MD) is the ratio of average modal bandwidth to average natural frequency spacing. If MD<0.2, modal parameter extraction depends on the frequency resolution of analysis system. If MD 0.2 to 1, modal parameter estimation depends on the precision and sophistication of the algorithms. If MD>1, structure's dynamics defy modal decomposition by signal processing techniques alone because of the inability to properly identity the No of modes to be extracted. Structure is assumed to be time invariant (no change with time).

3.2. Structure Mounting for Free-Free Boundary Conditions

A low carbon steel plate is mounted with the flexible bungees as shown in Figure 4 with the help of vertical stands so that free-free boundary conditions are simulated.

3.3. Experimental Model in Modal Software

A plate is modeled as per dimension in P-Win modal software [31] and marking of the 32 measurement points was made on model where accelerometers were mounted as shown in Figure 7.

It is normally done by a scaled layout drawing of the steel plate using digitizer table.

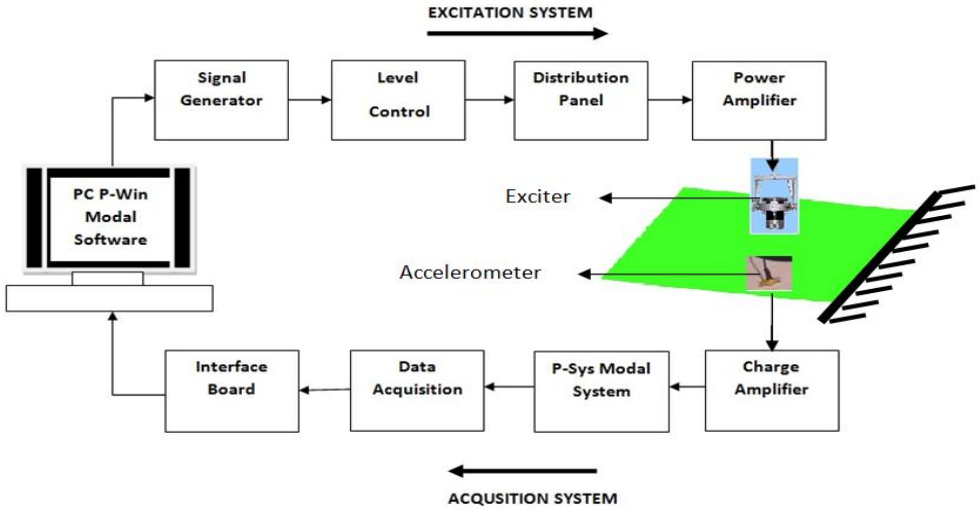

Figure 6. Schematic of experimental modal analysis.

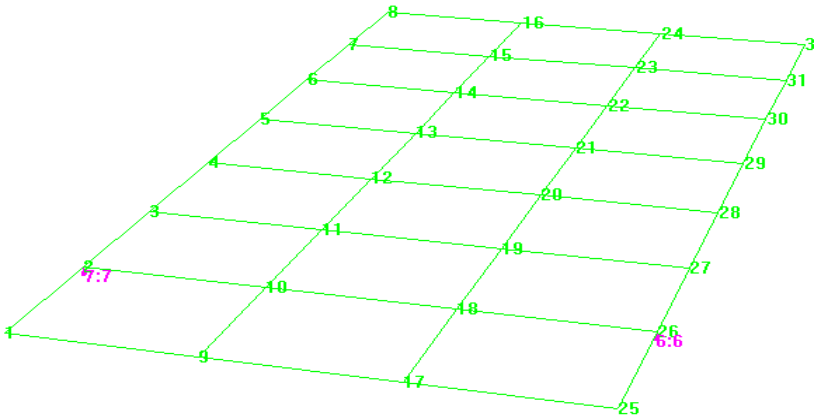

Figure 7. Plate in P-WIN modal software.

3.4. Transducer Calibration and Mounting on Plate

All transducers which are usually accelerometers are calibrated and mounted on the low carbon steel plate. The transducers for modal analysis tests are selected within the required magnitude and frequency limitations, avoiding relative motion between structure under test and the transducer, calibrating the complete measurement system to verify the performance and using uni-gain accelerometers that simplify monitoring of acceleration at several points on the structure. Piezo-resistive accelerometers are the best ones due to their less mass, low cost and acceptable time invariant measurement as shown in Figure 8.

Figure 8. Accelerometers.

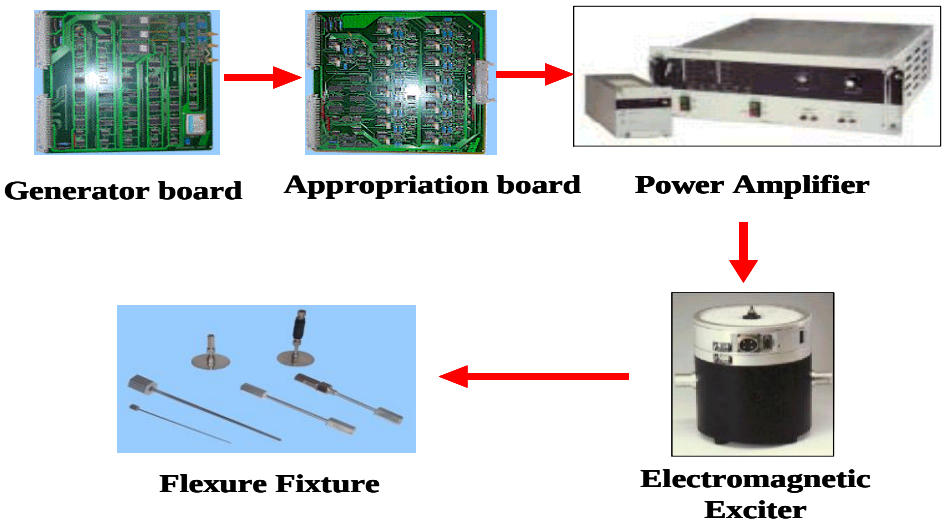

Figure 9. Test apparatus, generation and appropriation boards, power amplifier, exciter and flexure fixtures.

3.5. Installation of Excitation System

Excitation includes any form of input used to create a response in a mechanical system alongwith the environmental or operational inputs and the controlled force input (s) in GVT or modal analysis test as shown in Figure 6. The primary assumption concerning the excitement of a linear structure is that the measured characteristic properly describes the input characteristics.

There is a great deal of interest in determining turbulent air flow over an airfoil, road inputs to automobile and environmental inputs to proposed large space structures care must be taken not to confuse system resonances poles with those that exist in large spectrum due to inputs. Without force measurement it is not possible to know about the input to determine if the poles of the response are truly characteristics.

3.5.1. Exciters

Electromagnetic exciters shown in Figure 9 are used for an accurate control of the amplitude and phase of the force due to high dynamic range and constant force properties working on the principle of electromagnetic induction. If there are n degrees of freedom then “n” excites are required to identify all the possible modes. However, numbers of exciters are always limited and are positioned to extract the modes of interest only. Exciters’ natural frequencies must not lie within the required range of measurement and the exciters produce a reasonable response of the structure. Force may be roughly calculated [4] as follows in equation 4;

$$X' = F/m \times 2 \times \rho\,(2\Pi f)^{2} \qquad (4)$$

For frequency of 10 Hz, m = 100 kg and 2 % damping gives a displacement of about 6mm at 100 N force. Higher frequency modes are lighter than low frequency modes.

3.5.2. Mass Balance

Mass of the exciters is balanced using spring or elastic to avoid any addition of mass to the structure. However, exciter suspension system must be carefully selected for the required frequency range, because it is not possible to isolate at low frequency modes of 5 Hz or less using elastic and light exciter mountings. Heavy fixtures and spring of low stiffness, K may solve this problem.

3.5.3. Exciters Position

Nodal regions should be avoided and the extremities of free-free structure are generally a good choice. For exciting symmetrical modes, positioning of the shakers on the axis of symmetry is advisable and conversely should be avoided for anti-symmetrical modes. Since the aim of multiple exciter excitation is not only to excite the mode of interest but also to cancel the contribution from off resonant modes.

3.5.4. Power Amplifier

Power amplifier gives current in the output against a voltage signal produced by signal generation board as shown in Figure 9. The amplifiers are designed to operate in high impedance mode, where the output current is proportional to the input voltage with negligible shift.

3.5.5. Signal Generator

Metal structures have relatively low damping and often very close natural frequencies thus stable excitation of the modes places strict requirement on the generator which should have low distortion as harmonics components may excite undesired frequencies, High frequency resolution and low phase jitter to avoid side band around the excitation frequency.

3.6. Acquisition System

Acquisition system consists of transducers, signal conditioning and acquisition/switching boards. Signal conditioner gives output in volts/g and with selectable gain. Data acquisition cards, multiplier board and A/D cards are also a part of the signal processing system as shown in Figure 6. Output is received on computer on which final data analysis is done as shown in Figure 10.

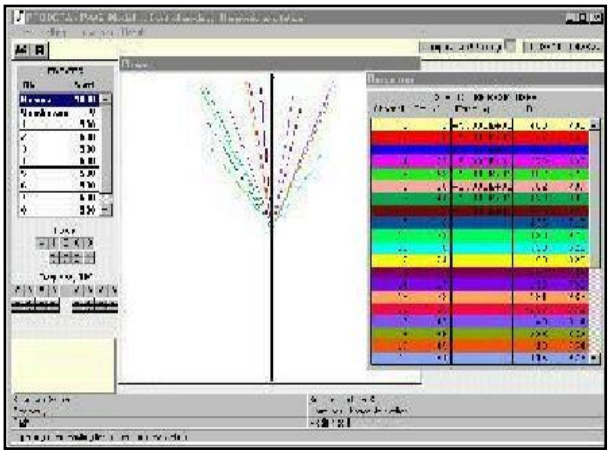

Figure 10. Data analysis.

3.7. Signal Processing

Primary concern in the modal data acquisition for formulation of modal digital signal processing i.e. conversion of analog signals in a corresponding sequence of digital values that accurately describe the time varying characteristics of the inputs to and responses from a system. There are two separate concepts related to dynamics performance of a digital processing analysis.

3.7.1. Sampling

The sampling is the process of recording the independent variable of an analog process, i.e., recording amplitudes at uniform increments of time (Δt) since all analogs to digital converters sample at constant sampling increments during which sample period. These are presented here [2] in the following sequence.

3.7.2. Nyquist Principle

$$f_N = fs/2 \quad (5)$$

where, fs is sampling frequency.

$$f_N \geq 2\times f(max) \quad (6)$$

where, f(max) is maximum frequency to be analyzed.

$$fs \geq 4\, f(max) \quad (7)$$

Nyquist frequency is the absolute maximum frequency below which aliasing error do not occur. Usually, fs = 5f (max).

3.7.3. Filter Selection

Generally bandwidth of the filter is approx 20% of Nyquist frequency. The filter is designed such that at Nyquist frequency the response is comparable to a single bit in the digital number representing the signal. For a 12 bit system one needs -66 db attenuation.

3.7.4. Frequency Resolution

Frequency resolution [2] is given by;

$$\Delta f = 1/T \quad (8)$$

At a frequency resolution of 0.2 Hz one must sample at least half of that in 10 seconds to acquire one ensemble of the test.

3.7.5. Quantization

Quantization is the conversion of specific analog value of amplitude to the nearest discrete value available in analog to digital conversion (ADC). This process represents a range of voltage by a fixed number of integer's steps. The number of discrete levels is a function of the number of bits in ADC. An ADC with n-bit convertor is able to determine signal amplitude within one part in 2 raised to n power [31].

4. Ground Vibration Testing Procedure and Results

The experimental model is prepared in P-Win-Modal software using 32 accelerometers and 2 exciters with seismic supports. Force appropriation method is used for the input excitations. An electro-magnetic exciter excites the structure with an impulse and harmonic force [32]. A flexure fixture is attached between the exciter and plate to transfer axial loads. The excitation is produced by a P-SYS model software code.

Dynamic signal analyzer sends the signals through an amplifier and transforms to a physical excitation by electro-magnetic exciter. The input forces are given by the exciters and the output motions are measured by the transducers attached to the plate with wax. Measurements are sent directly to the P-Win modal software to compute the frequency response for use in modal analysis. Complex power method calculates mode shapes, natural frequencies and damping ratios. The analysis found ten physical modes for the plate over a frequency range of 0 to 120 Hz.

4.1. Modal Data Presentation

Model consists of number of measurement points connected with one another to form links representing number of single degree of freedom system. Mode shape is the normalized response of the measurement point at the particular frequency better represented graphically. Mode shape can be represented either on 2-D structure in direction of co-ordinate axes with node lines distribution or simulated on a 3-D modal structure.

The first four experimental modes along with sensor meshing, first bending and first torsion are shown in Figures 11-20 respectively.

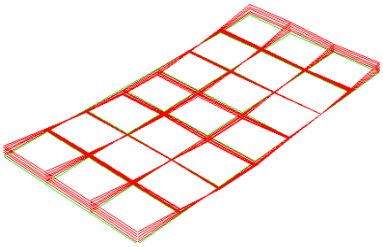

Figure 11. First Bending Mode (11.97Hz).

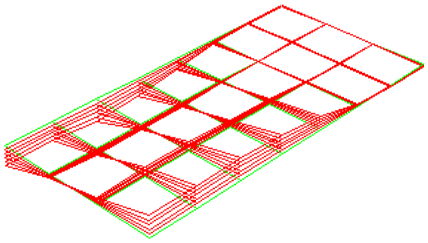

Figure 12. First Torsion Mode (15.47 Hz).

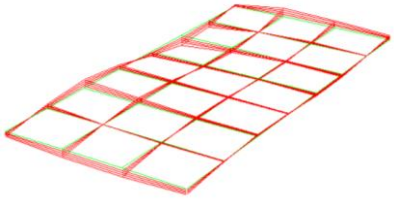

Figure 13. Asymmetric Torsion Mode (26.5 Hz).

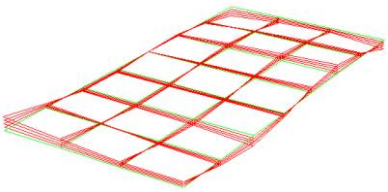

Figure 14. Second Bending Mode (32.347 Hz).

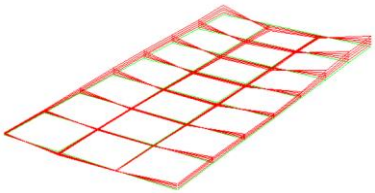

Figure 15. Second torsion mode (36.4 Hz).

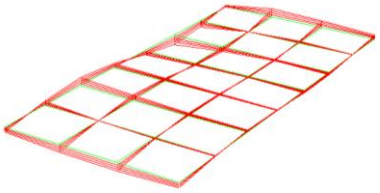

Figure 16. Asymmetric second bending mode (54.784 Hz).

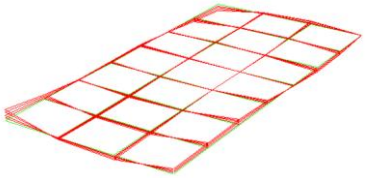

Figure 17. Symmetric second twist mode (59.906 Hz).

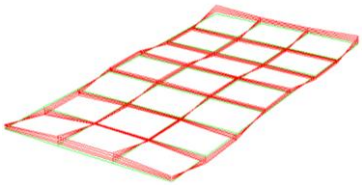

Figure 18. Symmetric third bending mode (67.925 Hz).

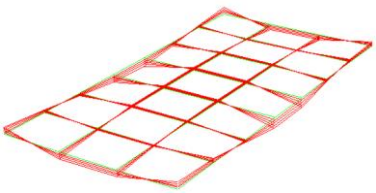

Figure 19. Symmetric third torsion mode (78.150 Hz).

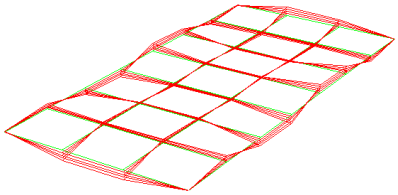

Figure 20. Asymmetric fourth bending mode (113.050 Hz).

Table 3. Experimental modal parameters.

Modes No.	Frequency (Hz)	Damping	Normalized generalized mass (Kg m^2)	Normalized generalized stiffness (Kg m^2/s^2)	Amplitude of reference transducer (m)
1	11.975	0.00906	31.018	1.7559725E+005	1.002251E-003
2	15.475	0.00426	14.869	3.5850287E+006	8.976649E-005
3	26.500	0.02965	27.310	7.5712543E+005	1.819537E-004
4	32.347	0.01087	45.486	1.8789087E+006	2.172576E-004
5	36.400	0.00445	100.033	5.2324475E+006	6.980755E-005
6	54.784	0.00746	6.571	7.7858500E+005	2.185061E-004
7	59.906	0.01200	4.784	6.7779143E+005	8.691209E-005
8	67.925	0.00378	22.116	4.0282450E+006	3.138889E-004
9	78.150	0.00426	14.869	3.5850287E+006	8.976649E-005
10	95.30	0.00108	24.280	1.2250256E+007	2.316853E-004

Experimentally determined mode shapes are also visually compared with numerical ones using MSC Nastran 2008 software [27]. Deform line representation is very helpful in making correction of measurement error e.g. defective or loose transducers. Response of the defective transducers may be adjusted by curve fitting techniques.

Complex power method estimates modal parameters using equations 9-10. Increase in real power and decrease in imaginary power shows the resonant frequency approach. Excitation condition is very important for modal analysis. The modal parameters of experimentally determined modes are shown in Table 3.

Normalized generalized mass [4].

$$= \{\Phi\}\{M\}\{\Phi\}=\{L\}\{M\}\{L\} \quad (9)$$

Normalized generalized stiffness [4]

$$= \{\Phi\}\{M\}\{\Phi\}=\{L\}\{[F]/[X]\}\{L\} \quad (10)$$

Where M is the mass in kg, L is the length in meters, F is the force in Newton and X is the displacement in meters.

4.2. Modal Data Validation

The identified and isolated quality of the modes is determined. Better the mode is isolated, better is the estimation of the modal parameters.

4.2.1. Orthogonality Test

Mode shapes should be orthogonal w. r. t. mass and stiffness matrices [4] i.e. for two modes r and s. With respect to Mass;

$$\{\Phi r\}\ \Phi\ [M]\ \{\Phi s\} = 1 \quad \text{if } r = s \quad (11)$$

$$\{\Phi r\}\ \Phi\ [M]\ \{\Phi s\} = 0 \quad \text{if } r \neq s \quad (12)$$

Ideally it should be diagonal matrix with off diagonal elements is equal to Zero and diagonal elements is equal to one.

With respect to Stiffness;

$$\{\Phi r\}\ \Phi\ [K]\ \{\Phi s\} = 1 \quad \text{if } r = s \quad (13)$$

$$\{\Phi r\}\ \Phi\ [K]\ \{\Phi s\} = 0 \quad \text{if } r \neq s \quad (14)$$

Practically off diagonal elements are not zero and as per MIL-A-8870C [33], 10% deviation is considered acceptable. High value of off diagonal elements shows the following problems in the experimental testing.

Table 4. Modal assurance criteria (MAC).

Modes	1	2	3	4	5	6	7	8	9	10
1	100	-	-	-	-	-	-	-	-	-
2	0.601	100	-	-	-	-	-	-	-	-
3	0.099	30.86	100	-	-	-	-	-	-	-
4	0.150	5.322	6.085	100	-	-	-	-	-	-
5	0.211	2.704	15.96	33.44	100	-	-	-	-	-
6	1.770	0.342	0.103	2.619	2.720	100	-	-	-	-
7	0.052	0.349	0.003	0.990	2.081	0.635	100	-	-	-
8	11.86	0.047	0.002	0.313	0.269	0.138	0.45	100	-	-
9	2.777	0.151	0.001	0.089	0.001	0.008	0.086	3.801	100	-
10	0.099	0.003	0.000	0.014	1.399	0.029	0.645	0.020	0.017	100

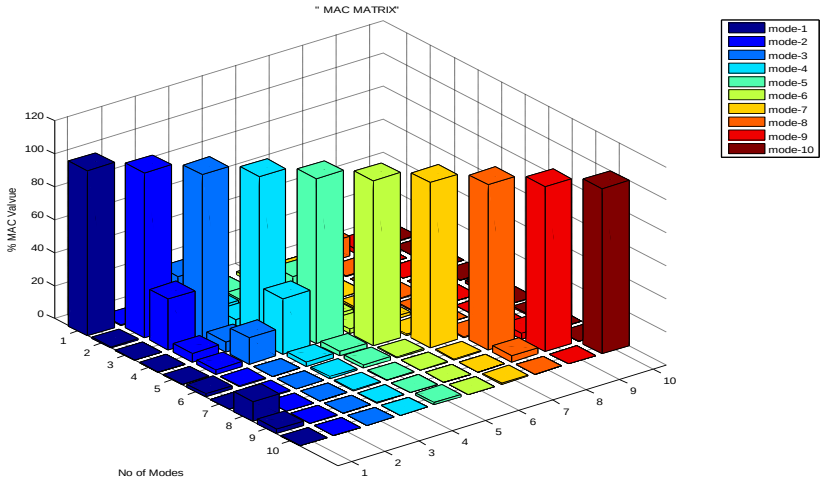

Figure 21. Modal assurance criteria (MAC).

1. Inadequate test model, DOF are too low or measurement points are not optimal.
2. Mode shapes originate from operational forces are not from resonances.
3. Non stationary conditions.
4. Non linear conditions.
5. Orthogonality property is not fulfilled.

The test requires mass and stiffness matrices which is not usually available for the most cases, therefore, modal assurance criteria (MAC) as a close approximation are used.

4.2.2. Modal Assurance Criteria (MAC)

Modal assurance criterion checks how well the modes are extracted and isolated. It determines the linear dependence of the mode shapes [4]. It is stated that for perfectly isolated modes r and s;

$$MAC = |\{\Phi r\}^T \{\Phi s\}|^2 / (\{\Phi r\}^T \{\Phi s\}) (\{\Phi s\}^T \{\Phi r\}) \quad (15)$$

$$MAC = 0 \text{ if } r \neq s \text{ and } MAC = 1 \text{ if } r = s \quad (16)$$

The experimental extracted modes are checked for their Orthogonality just after the test to remove off diagonal elements while the test is still running that might lead to error. Modal assurance criterion checks the correlation between different experimentally determined modes for Orthogonality as shown in Table 4 and Figure 21.

Table 5. Comparison of Numerical & Experimental data.

No.	Modes	Numerical results (Hz)	Experimental results (Hz)
1	1	12.80	11.975
2	2	15.738	15.475
3	3	25.7	26.500
4	4	34.44	32.347
5	5	35.534	36.400
6	6	51.86	54.784
7	7	60.155	59.906
8	8	70.702	67.925
9	9	86.051	78.150
10	10	94.969	95.3

Table 6. Different cases with respect to structural defects.

Cases	Structural defect	Justifications
1	No crack	Ideal Structure
2	Multiple cracks (Random)	Manufacturing, fatigue and other reasons.
3	Multiple cracks & holes (Random)	Material deterioration and pitting, bullet fired by an anti aircraft gun on wing
4	Multiple cracks, holes & symmetric lumped masses	Two Store are attached at the Wing Stations
5	Multiple cracks, holes & asymmetric lumped masses	If one store is fired and other store is still at the wing station

Ideally, normal modes are orthogonal i.e. having Zero MAC values and correlations with each other. Practically, it is difficult to achieve completely isolated modes but, maximum orthogonal criteria could be achieved.

5. Comparison of Numerical and Experimental Results

Numerical and experimental results are analyzed as shown in Table 5.

Some differences in the values are due to the non-homogeneous distribution of low carbon steel plate material and homogeneous nature of numerical model. For the sake of comparison it is concluded that numerical modal analysis results are well in agreement with experimental data.

The eigenvalues and eigenvectors are dependent on the stiffness and the mass distribution of the structure. During material manufacturing process the stiffness of the batch varies slightly due to the process control and micro flaws in the material structures affecting the eigenvalues and eigenvectors of that particular structure. It is quite evident from Table 5 that modal frequency of numerical and experimental results vary a little bit but the eigenvectors remain the same. Table 5 shows change in frequency due to flaws in manufacturing process subsequently changing the eigenvalues and eigenvector and ultimately change the stiffness of the structures.

The dependency of the stiffness and mass distribution on the modal frequency is further studied on large scale due to different flaws in the structure as given in Table 6. Their frequency shift due to different flaws is investigated numerically in MSC Nastran 2008 and experimentally by considering first four modes i.e. first bending, first torsion, second bending and second torsion.

In case 1, an ideal plate is considered with the assumption that no crack exists. This ideal plate is used as a reference for comparing the results of all other cases in which flaws were induced later on. In case 2, multiple cracks are induced in the structure which might be due to manufacturing, fatigue and other reasons. In case 3, alongwith multiple cracks as mentioned in the case 2, multiple holes are also induced in the same plate which might be due to material deterioration and pitting or a structure being fired by an anti aircraft gun. In case 4, alongwith multiple cracks and multiple holes, symmetric masses of 10 Kg each are added on lower left and right sides of the plate to simulate a wing with two stores attached at different stations. Lastly in case 5, alongwith multiple cracks and multiple holes, asymmetric mass of 10 Kg is present on the lower left side of the plate to simulate a wing with one store fired and one is still at the wing station. These cases show the worst case scenario by the addition of flaws and effect of symmetric and asymmetric configurations. Numerical mode shapes from MSC Nastran for case 1 to case 5 are shown in Figures 22 - 26 respectively.

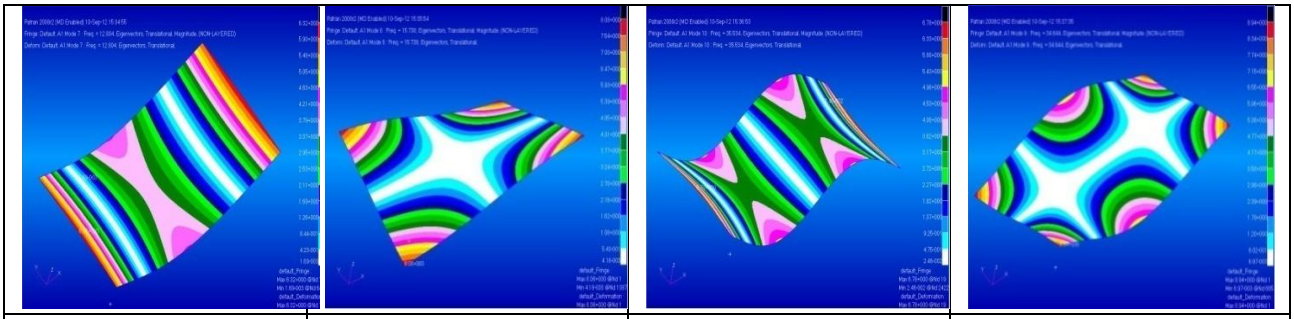

Mode 1: Bending	Mode 2: 1st Torsion	Mode 3: 2nd Bending	Mode 4: 2nd Torsion

Figure 22. Modes shapes for case 1.

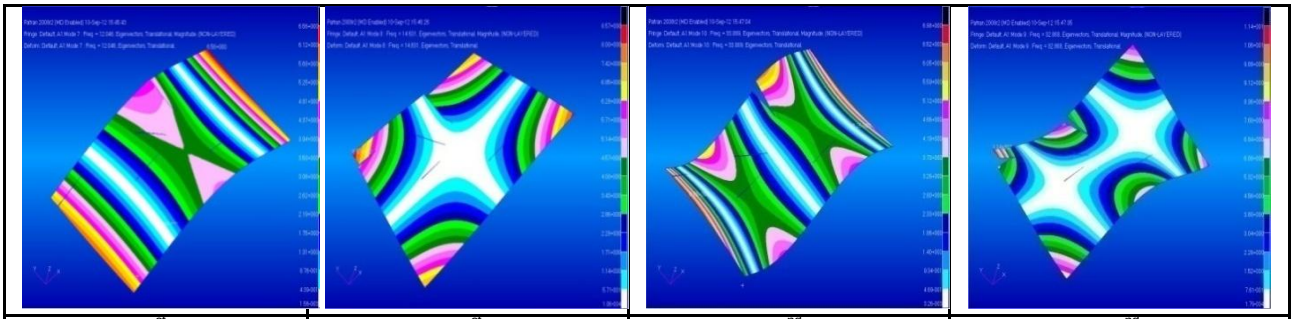

Mode 1: 1st Bending	Mode 2: 1st Torsion	Mode 3: 2nd Bending	Mode 4: 2ndTorsion

Figure 23. Modes shapes for case 2.

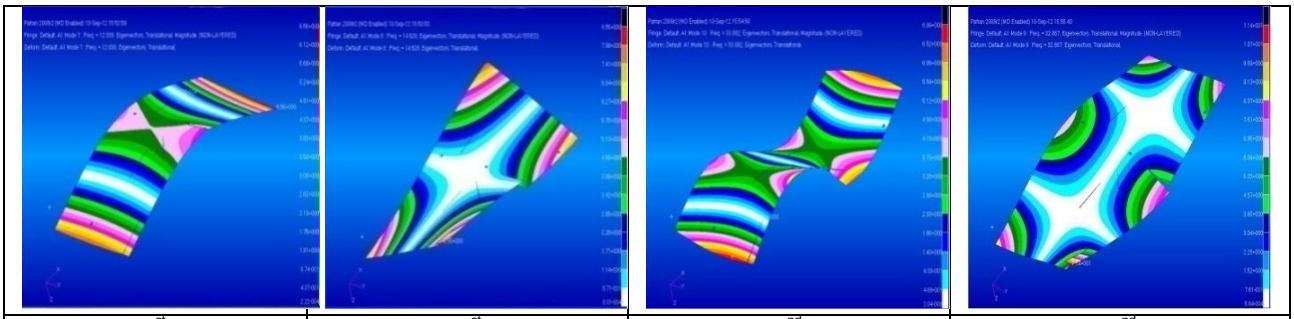

Mode 1: 1st Bending	Mode 2: 1st Torsion	Mode 3: 2nd Bending	Mode 4: 2nd Torsion

Figure 24. Modes shapes for case 3.

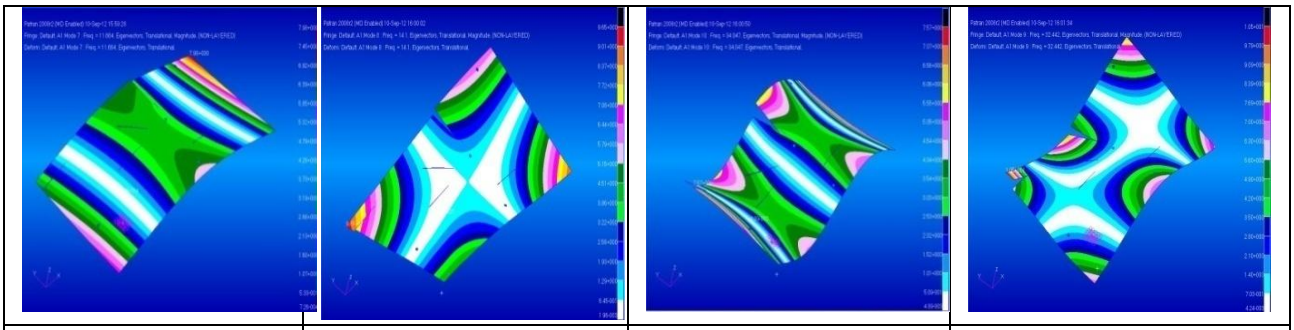

Mode 1: 1st Bending	Mode 2: 1st Torsion	Mode 3: 2nd Bending	Mode 4: 2nd Torsion

Figure 25. Modes shapes for case 4

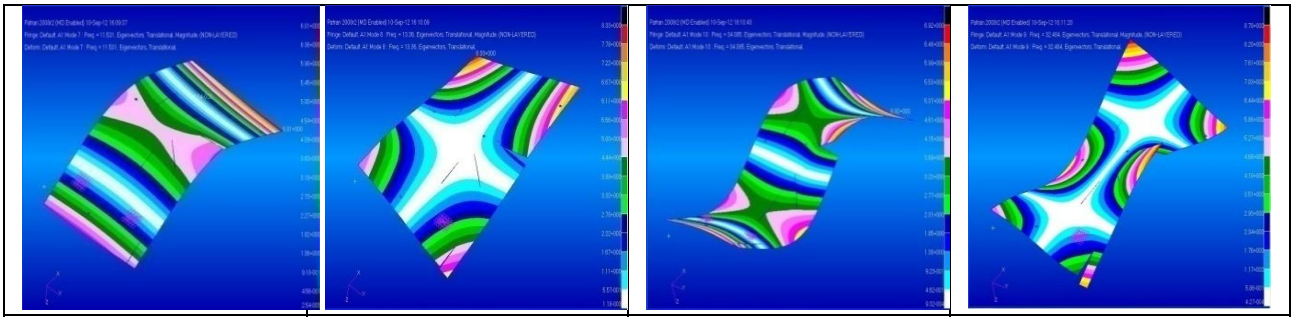

Mode 1: 1st Bending	Mode 2: 1st Torsion	Mode 3: 2nd Bending	Mode 4: 2nd Torsion

Figure 26. Modes shapes for case 5.

Percentage frequency shifts are determined by comparing numerical natural frequencies with the numerical ideal plate and experimental natural frequencies with the experimental ideal plate respectively in each case mentioned in Tables 7a, 7b, 7c & 7d. It is observed that the frequency shift also increases with the increase in the number of flaws.

Percentage frequency shift for all numerically computed and experimentally determined results with reference to the ideal plate with no crack numerically are shown in the Tables 8a, 8b, 8c & 8d.

It is observed that symmetric lumped masses scenario is the worst among all and it must be analyzed critically in structural dynamic analysis as compared to asymmetric lumped masses. In mode 1 it is observed that % shift in frequency increases as the flaws are added to the structure from 13.3 to 21.1, similarly in modes 2~4 %shift in frequency increase from 10.78 to 25.08,5.72 to 6.50 and 11.53 to 15.20 respectively. It is quite clear that the natural frequency decreases with decrease in the stiffness due to increase in the number of flaws.

6. Discussion and Analysis

Modes are greatly affected by material and structural flaws because it changes the modal parameters. To see the impact of these flaws in a sequence from a clean configuration to a combination of number of uncertainties in an isotropic material, a simple low carbon steel plate is taken. Experimental and numerical modal analysis is performed on this plate. Ideally, a perfect model would match all experimental and numerical modes while in actual, it is not expected because of manufacturing and environmental conditions. Material and structural flaws are step by step added to see the cumulative variation in stiffness parameters and their effects on four critical modes; first bending, first torsion, second bending and second torsion. A notable percentage shift is observed in the modal frequency, which shows that by adding the number of flaws the stiffness of the structures changes. Experimental and numerical results showed considerable closeness which verified the procedures adopted. This showed the importance of delicacies adopted in this study to minimize the future experimental errors in modal analysis. Highest percentage shift is observed in case 5 of multiple cracks, holes & asymmetric lumped masses addition as in Table 8d.

Table 7a. Frequency shift by comparing case 1 and case 2

Modes	Numerical			Experimental		
	Case 1 (Hz)	Case 2 (Hz)	Percentage Frequency Shift	Case 1 (Hz)	Case 2 (Hz)	Percentage Frequency Shift
1	12.804	12.046	5.9	11.975	11.10	7.3
2	15.738	14.631	7.03	15.475	14.04	9.2
3	35.534	33.889	4.62	36.4	33.5	7.96
4	34.644	32.868	5.12	32.347	30.65	5.2

Table 7b. Frequency shift by comparing case 1 and case 3.

Modes	Numerical			Experimental		
	Case 1 (Hz)	Case 3 (Hz)	Percentage Frequency Shift	Case 1 (Hz)	Case 3 (Hz)	Percentage Frequency Shift
1	12.80	12.038	5.98	11.975	11	8.14
2	15.738	14.628	7.05	15.475	13.8	10.8
3	35.534	33.882	4.65	36.4	33.2	8.79
4	34.644	32.867	5.13	32.347	30.1	6.94

Table 7c. Frequency shift by comparing case 1 and case 4

Modes	Numerical			Experimental		
	Case 1 (Hz)	Case 4 (Hz)	Percentage Frequency Shift	Case 1 (Hz)	Case 4 (Hz)	Percentage Frequency Shift
1	12.804	11.664	8.903	11.975	10.7	10.64
2	15.738	14.1	10.41	15.475	13.1	15.3
3	35.534	34.047	4.18	36.4	33.1	9.06
4	34.644	32.442	6.35	32.347	29.4	9.1

Table 7d. Frequency shift by comparing case 1 and case 5

Modes	Numerical			Experimental		
	Case 1 (Hz)	Case 5 (Hz)	Percentage Frequency Shift	Case 1 (Hz)	Case 5 (Hz)	Percentage Frequency Shift
1	12.804	11.531	9.942	11.975	10.1	15.6
2	15.738	13.36	15.1	15.475	11.8	23.75
3	35.534	34.085	4.07	36.4	33.2	8.8
4	34.644	32.484	6.23	32.347	29.35	9.26

Table 8a. Frequency shift by comparing numerical case 1 and experimental case 2.

Modes	No Crack (Numerical) (Hz)	With Multiple Cracks (Experimental) (Hz)	Percentage Frequency Shift
1	12.804	11.10	13.3
2	15.738	14.04	10.78
3	35.534	33.5	5.72
4	34.644	30.65	11.53

Table 8b. Frequency shift by comparing numerical case 1 and experimental case 3.

Modes	No crack (Numerical) (Hz)	With Multiple Cracks & Holes (Experimental)(Hz)	Percentage Frequency Shift
1	12.804	11	14.08
2	15.738	13.8	12.3
3	35.534	33.2	6.568
4	34.644	30.1	13.11

Table 8c. Frequency shift by comparing numerical case 1 and experimental case 4

Modes	No Crack (Numerical) (Hz)	With Multiple Cracks, Holes & Asymmetric Mass (Experimental) (Hz)	Percentage Frequency Shift
1	12.804	10.7	16.43
2	15.738	13.1	16.76
3	35.534	33.1	6.85
4	34.644	29.4	15.1

Table 8d. Frequency shift by comparing numerical case 1 and experimental case 5

Modes	No crack (Numerical) (Hz)	With Multiple Cracks, Holes & Symmetric Mass (Experimental) (Hz)	Percentage Frequency Shift
1	12.804	10.1	21.1
2	15.738	11.8	25.02
3	35.534	33.2	6.5
4	34.644	29.35	15.2

Another interesting and important result is observed while the delta between the first bending and first torsion is calculated. With the induction of material flaws like cracks and holes, delta starts to decrease. This decrease is more significant when the symmetric and asymmetric stores configuration is coupled with these flaws. The delta of the first two modes in clean configuration is 3.031 Hz numerically and 3.50 experimentally as shown in Table 9.

Table 9. Comparison of first bending mode and first torsion mode with delta both numerically and experimentally.

Sr. No.	Cases	Numerical			Experimental		
		Bending Modes (Hz)	Torsion Modes (Hz)	Delta (Hz)	Bending Modes (Hz)	Torsion Modes (Hz)	Delta (Hz)
1	Case 1	12.829	15.860	3.031	11.975	15.475	3.5
2	Case 2	12.046	14.631	2.585	11.10	14.04	2.94
3	Case 3	12.038	14.628	2.59	11.00	13.8	2.80
4	Case 4	11.664	14.1	2.436	10.7	13.1	2.4
5	Case 5	11.531	13.36	1.829	10.1	11.8	1.70

This delta keeps on decreasing in case 2 and case 3. In asymmetric configuration, when mass is added the delta decreases to 2.436 Hz numerically and 2.40 Hz experimentally. In symmetric configuration when masses are added, the delta decreases to 1.829Hz numerically and 1.70 Hz experimentally that is even worse than asymmetric configuration. Due to small delta, certain modes may start converging with the increase of air speed due to some aeroelastic effects which may result in dynamic instability. Possible coupling of the critical modes occurs at a relatively higher speed due to the small delta of the modes, sometimes this phenomenon is predicted in unsteady aerodynamic analysis results at such equivalent air speed that could not be achieved in given Mach number with real atmospheric conditions.

This study is very important and interesting for reduction of experimental activities during qualification phases of structures. However, a lot of research work is still required before any concrete conclusion. Location of the masses, holes and cracks on the plate has a significant effect on the dynamic properties and would be investigated further.

7. Conclusion

As a result of the experimental and numerical studies following conclusions are made:

- Modal parameters of structures changes due to the material flaws like cracks, holes, mass distribution (Asymmetric and Symmetric) and manufacturing processes.
- By comparing individually each flaw it shows less uncertainty in results but by combining all mentioned flaws it is evident that uncertainty increases a lot which might affect the structure in its service life. By using this research for the isotropic material, designer can well estimate the affect of individual and cumulative uncertainties.
- Although the difference in the respective modes in different cases looks small in digits, but it term of percentages it had the significance affect. This percentage is at its peak value in case of flaws plus symmetric masses case.
- From the results, it may be safely concluded that Symmetric configuration is the worst as comparing with asymmetric configuration. This case study show that Flaws in the material may cause the structures more venerable to flutter in the numerical prediction analysis as they have tendency to couple together quickly due to less frequency shift and tendency of lower damping. A lot of time and money may be saved by reducing the number of configurations to be investigated in Ground Vibration Testing (GVT) an extensive activity and first step towards the flutter qualification procedure and by keeping in mind the delicacies for experimental modal analysis explained in this paper which is based on the true experience.
- First bending and first torsion are of extreme importance in case of dynamic aeroelastic analysis (Flutter). As frequency shifts, It effects the aeroelastic analysis i.e. flutter speed of the structure. Delta in first two modes in this study reveals that frequencies for symmetric configuration are approaching to each other which may cause flutter. It will be studied in future in detail.
- The comparison of Numerical and Experimental results gives the fair idea of accuracies of the results obtained from

numerical simulation and experimental results along with justification provided in this research.

- Taking into account the delicacies mentioned in this research gives the closeness of numerical and experimental results due to inherent problems in both.
- It is also observed that cracked structures give different frequencies as compared to clean structures. However, flutter prediction of cracked and flawed materials may differ on the basis of crack and flaw size and its orientation. It is therefore important to calculate accurate flutter speed because of catastrophic behavior and if possible both flutter speeds should be computed i.e. with or without flaws and should be given speed range in term of upper flutter speed and lower flutter speed rather than a single flutter speed.

References

[1] M. Nuno, M. Maia, M. Julioand M. Silva, Theoretical and Experimental Modal Analysis, RSP, England (1998).

[2] F.S. Tse, I.E. Morse Jr. and R.T. Hinkle, Mechanical Vibrations: Theory and Applications, 2nd Edition, Prentice-Hall, Inc., Englewood Cliffs, New Jersy (1978) pp 449

[3] R.R. Craig Jr., Structural Dynamics: An introduction to computer Methods, John Wiley & Sons, Inc,New York (1981) pp.527.

[4] D. Ewans, Modal Testing: Theory and Practice, John Wiley & Sons, Inc., New York (1984) pp.269.

[5] J.S. Bendat and A.G. Piersol, Random Data, Analysis and Measurement Procedures, John Wiley & Sons, Inc., New York (1984) pp.269.

[6] D. Ewans, Modal Testing: Theory and Practice, John Wiley & Sons, Inc, New York (1971)pp.407.

[7] D. Ewans, Engineering Applications of Correlation and Spectral Analysis, John Wiley & Sons, Inc., New York (1980)pp.302.

[8] R.K. Otnes and L. Enochson, Digital Time Series Analysis, John Wiley & Sons, Inc., New York (1972) pp.467.

[9] Jim He and Zhi-Fang-Fu., Modal Analysis, Butterworth-Heinemann, U.K. (2001).

[10] K.G. McConnell and P.S. Varoto, Vibration Testing: Theory and Practice, John Wiley & Sons, Inc., New Jersy, Canada (2008).

[11] H. Ashley, Aeroelasticity, Applied Mechanics Reviews **23** (1970) 119.

[12] R.L. Bisplinghoff, H. Ashley and R.L. Halfman, *Aeroelasticity,* Addison-Wesley Publishing Company, Reading, Mass (1955).

[13] Y.C. Fung, An Introduction to Theory of Aeroelasticity, John Wiley & Sons, Inc, New York, 1955.

[14] R. Marissen, "Fatigue Crack Growth prediction in Aramid Reinforced Aluminum Laminates(ARALL)", Journal of Aircraft **25**, No. 2 (1988) 135.

[15] G.C. Sih and E.P. Chen, "Cracks in Composite Materials", Mechanics of Fracture **6** (1981) 26.

[16] Lin Kuo-Jiun, Lu Pong-Jeu and Jiann-Quo Taint, "Flutter Analysis of Anisotropic Panels with Patched Cracks" Journal of Aircraft **28**, No. 12 (1991) 899.

[17] R.M. Verette and E. Permits, Army Material and Mechanics Research Center **MS 76-Z** (1976) pp.123-136.

[18] D.R. Perchard and A.S.J. Swamidas, Crack detection in Slender Cantilever Plates using Modal Analysis", 12th International Modal Analysis Conference **2**, Hawaii, USA. (1971), pp. 1769-1777.

[19] R. Solecki, International J. of Engg. Sci. **18** (1980) 1309.

[20] R. Solecki, Engineering Fracture Mechanics **18** (1983) 1111.

[21] R. Solecki, Engineering Fracture Mechanics **22** (1985) 687.

[22] S. H. Yoo and H.K. Kwak, Detection and Location of a Crack in a Plate Using Modal Analysis, 17th International Modal Analysis Conference **3727** (1999) pp. 1902-1920.

[23] J. E. Kim, S. H. Yoo and E. J. Park, On Detecting a Crack in a Plate by the Change of Modal Parameters, Proceedings of the KSME Spring Annual Meeting (1998) pp. 408-413.

[24] T. Wolff and M. Richardson, Fault Detection in Structures from Changes in Their Modal Parameters, 7th IMAC (1989) pp. 87-94.

[25] L. D. Mitchell, Increasing the Sensitivity of the Modal Assurance Criteria (MAC) to Small Mode Shape Changes: The IMAC, 16th IMAC (1997) pp. 64-69.

[26] R. Kolar, Modal Analysis and Damage Assessment of Cracked Plates, NASA

Dryden Flight Research Center, Dryden, California.

[27] MSC.Software Manuals for MSC.Nastran/ Patran (a) MSC.Patran User's Guide. (b) MSC.Patran Reference Manual, Part 1-7, (c) MSC Advanced Dynamic Analysis, (d) MSC.Patran User's Guide, (e) MSC.Nastran Aeroelastic Analysis User's Guide, (f) MSC.Patran FlightLoads and Dynamics User's Guide, (g) MSC.Nastran Quick Reference Guide, (h) MSC.Nastran Basic Dynamic Analysis Users Guide, UGS Corp. (2008).

[28] M. Leonard, Principle and Technique of Vibrations, Printine Hall, New Jersey (1997) pp.401.

[29] K. Zaveri, Modal Analysis of Large Structures, 1st Edition (May 1984) pp.75.

[30] J.S. Bendat and A.G. Piersol, Analysis and Measurement Procedures, John Wiley and Sons, New York (1971) pp.407.

[31] National Instruments, Measurement and Automation Catalogue (2001) pp.244.

[32] E. Balmes et al., An Evaluation of Modal Testing Results Based on the Force Appropriation Method ONERA TP, Proc. IMAC (1995) pp. 1-7

[33] USAF Military Specifications, MIL-A-8870C, Military Specification: Airplane Strength and Rigidity Vibration, Flutter and Divergence (1993).